Catal Lett (2009) 129:142–148
DOI 10.1007/s10562-008-9797-6

Optimization of Synthesis Gas Formation in Methane Reforming with Carbon Dioxide

Beata Michalkiewicz · Joanna Sreńscek-Nazzal · Janusz Ziebro

Received: 2 July 2008 / Accepted: 20 November 2008 / Published online: 11 December 2008

Abstract The carbon dioxide reforming of methane over Ni/SiO_2, $Ni–Co/SiO_2$ and commercial nickel catalyst was investigated. The best methane conversion (57%) and H_2 (53%) yield were achieved over Ni industrial catalyst. This catalyst, however, undergoes deactivation as a result of carbon formation. The advantage of the bimetallic catalysts is high resistance to metal reduction and coking.

Keywords $CH_4 \cdot CO_2 \cdot$ Reforming · Catalyst · Nickel · Copper · Syngas

1 Introduction

The conventional method for synthesis gas production is the steam reforming of methane.

$$CH_4 + H_2O \rightleftarrows CO + 3H_2 \quad \Delta H = +206\,\mathrm{kJ/mol} \qquad (1)$$

This reaction is operated industrially at 730–850 °C under 2–4 MPa. Alumina supported nickel catalyst has been used usually.

Recently much attention has been paid to methane reforming with carbon dioxide:

$$CH_4 + CO_2 \rightleftarrows 2CO + 2H_2 \quad \Delta H = +247\,\mathrm{kJ/mol}. \qquad (2)$$

The reaction of carbon dioxide reforming of methane to produce synthesis gas has attracted interest from both environmental and industrial perspectives. The environmental viewpoint stem from the fact that both CO_2 and CH_4 are viewed as harmful greenhouse gases. CO_2 reforming of CH_4 convert the two greenhouse gases into a valuable feedstock: synthesis gas. CH_4 and CO_2 are relatively inexpensive.

A quick deactivation of the catalysts used in the process can be the result of carbon deposition on the catalyst. Carbon deposition is, in fact, a serious problem affecting the catalysts of methane reforming with CO_2 [1–3]. Nickel on various carriers, such as SiO_2 [4–6], Al_2O_3 [2, 7–9], TiO_2 [10–13], MgO [14–16] were described as the most effective catalysts of dry reforming. However, the speed of carbon and deposition formations on nickel catalysts is much higher than that in systems containing noble metals [14]. Platinum, rhodium, palladium and ruthenium catalysts [17–21] are much more stable, but due to their high prices it is advisable to obtain active and stable catalysts which do not contain noble metals.

Nickel is one of the most frequently investigated metals in CH_4 dry reforming. Its most important advantage is high reactivity, accessibility and low price. Conversely, its main drawback is poor resistance toward carbon deposition and that is why much effort in the previous research was focused on an in-depth understanding and limiting of this phenomenon [8, 22]. That is why efforts to search for stable nickel catalysts were undertaken. A modification of nickel catalysts is achieved mostly by applying an appropriate carrier [7, 23, 24] as well as by using special methods of preparation [22, 25] or by means of using bimetallic systems. An application of bimetallic systems results in an increase of the stability and activity of nickel catalysts used in methane reforming with carbon dioxide [23, 25, 26]. An addition of copper into the nickel catalyst seated

B. Michalkiewicz (✉) · J. Sreńscek-Nazzal · J. Ziebro
Institute of Chemical and Environment Engineering, Szczecin University of Technology, ul. Pulaskiego 10, 70-322 Szczecin, Poland
e-mail: beata.michalkiewicz@ps.pl

J. Sreńscek-Nazzal
e-mail: jsrenscek@ps.pl

on SiO_2 carrier is conducive to the reaction of CH_4 with CO_2 leading to a great increase of this catalyst's stability [23].

Table 1 Composition of the studied catalysts

Catalyst	Ni [wt%]	Cu [wt%]
Ni(10)/SiO_2	10	–
Ni(10)–Cu(1)/SiO_2	10	1
Ni(10)–Cu(3)/SiO_2	10	3
Ni industrial	16	–

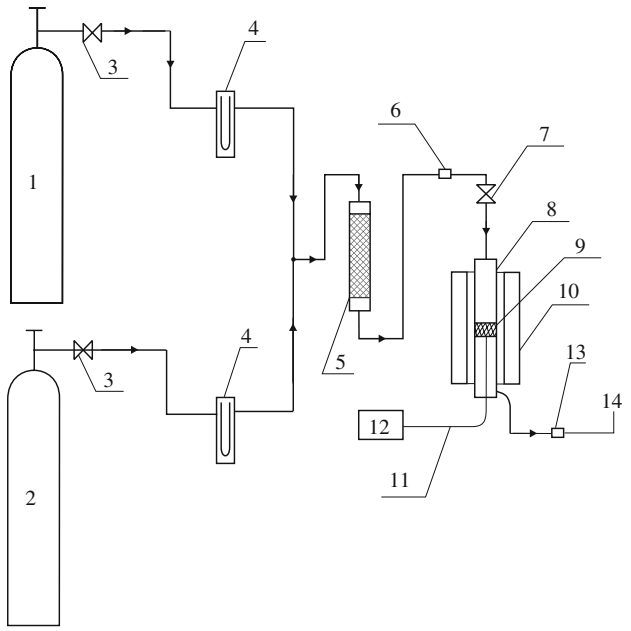

Fig. 1 Schematic diagram of reaction set-up for the methane reforming with carbon dioxide: 1-bottle with CH_4, 2-bottle with CO_2, 3-micrometric valve, 4-flowmeter, 5-mixer of gases, 6-membrane to taking the samples of gases, 7-valve, 8-reactor, 9-bed of catalyst, 10-oven, 11-thermocouple, 12-thermoregulator, 13-membrane to taking the samples of products, 14-vent

Table 2 Surface area (BET) and pore volume of the catalysts

Sample	S_{BET} (m^2/g)	V_{tot} (cm^3/g)
Ni(10)/SiO_2 before reaction	297.2	0.289
Ni(10)/SiO_2 after reaction (550 °C)	184.2	0.201
Ni(10)–Cu(1)/SiO_2 before reaction	303.9	0.294
Ni(10)–Cu(1)/SiO_2 after reaction (550 °C)	234.1	0.236
Ni(10)–Cu(3)/SiO_2 before reaction	296.7	0.285
Ni(10)–Cu(3)/SiO_2 after reaction (550 °C)	264.07	0.265
Ni industrial before reaction	4.5	0.013
Ni industrial after reaction (550 °C)	18.7	0.028

V_{tot}, total pore volume

The present study shows the results of investigations concerning the possibilities of using nickel catalysts, and especially using a commercial nickel catalyst employed in the conventional processes of synthesis gas production. The process was carried out under atmospheric pressure. The carbon deposit obtained as a result of methane reaction with CO_2 was characterized using XRD and SEM methods.

2 Experimental

The properties of the obtained nickel catalysts were studied by means of different methods. To determine the pore volumes, N_2 sorption isotherms were found at −196 °C

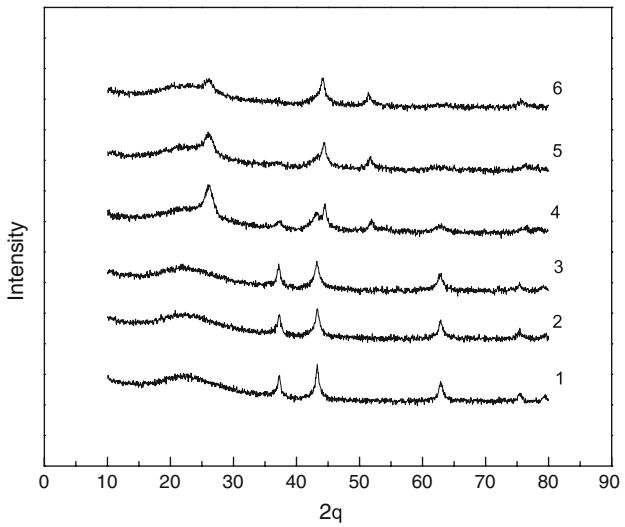

Fig. 2 X-ray diffraction patterns of prepared catalysts. Co K_α radiation. 1-Ni(10)/SiO_2 before reaction, 2-Ni(10)–Cu(1)/SiO_2 before reaction, 3-Ni(10)–Cu(3)/SiO_2 before reaction, 4-Ni(10)/SiO_2 after reaction, 5-Ni(10)–Cu(1)/SiO_2 after reaction, 6-Ni(10)–Cu(3)/SiO_2 after reaction

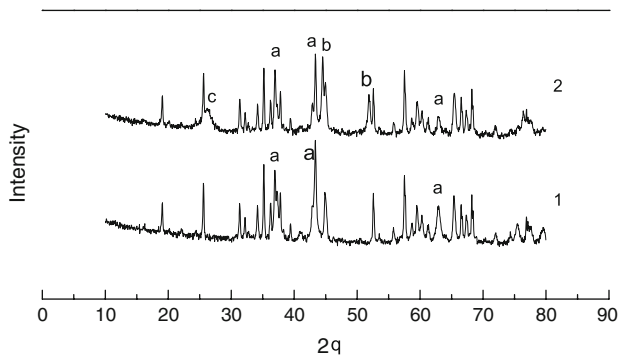

Fig. 3 X-ray diffraction patterns of Ni industrial. Co K_α radiation. 1-Ni industrial before reaction, 2-Ni industrial catalyst after reaction. *a* NiO, *b* Ni, *c* graphite

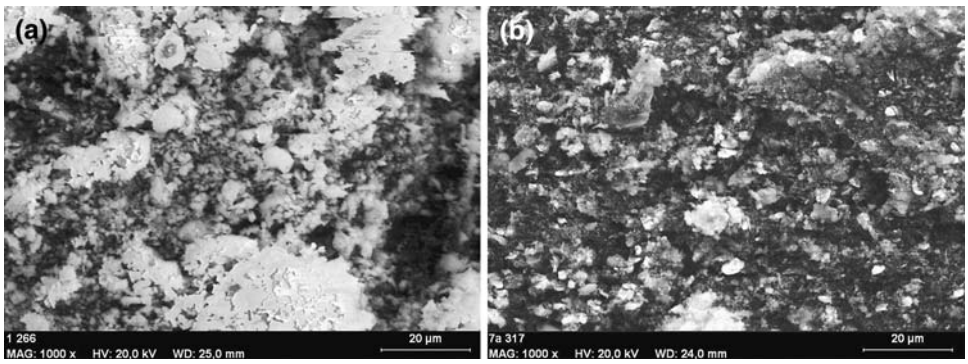

Fig. 4 SEM picture of Ni industrial catalyst **a** before and **b** after reaction (at 550 °C) taken at magnification of ×1000

using ASAP 2010 apparatus (Micromeritics). The samples were previously evacuated at 250 °C for 16 h. The BET method was used to calculate the surface area (S_{BET}) of the samples, while the micropore volume (V_{micro}) was determined using the *t*-plot method.

A direct observation of the catalysts morphology was carried out by means of energy-dispersive X-ray spectroscopy (EDS) XFlash 4010—Bruker AXS using a scanning electron microscope DSM 962—ZEISS.

The phase compositions of the catalyst' samples were investigated using X-ray diffractometry (XRD) with Phillips instrument. Cobalt tube and scanning rate 1°/min at room temperature were used. Crystalline phases were identified by comparing them with ICDD reference files.

The carrier used to prepare the catalysts was SiO_2 whose BET area amounted to 500 m^2/g. All the investigated nickel systems were obtained through the impregnation of SiO_2 with an aqueous solution of $Ni(NO_3)_2{\cdot}6H_2O$. Copper was introduced as $Cu(NO_3)_2{\cdot}3H_2O$. The nickel contacts included 10 wt% Ni and 1 and 3% Cu for Ni–Cu/SiO_2 bimetallic catalysts. The suspension of the catalyst's precursors was agitated for 5 h in a vacuum evaporator and the pressure was lowered by 830 hPa. The samples were dried at 105 °C for 8 h and later calculated for 6 h at 600 °C. The catalyst was formed as grains with an appropriate diameter. An industrial nickel catalyst was also subjected to catalytic tests of dry reforming. This catalyst is used in steam methane reforming processes and contains also aluminum oxide and promoters. The data about the tested catalysts are presented in Table 1.

The catalytic reaction of methane reforming with carbon dioxide was performed under atmospheric pressure in a quartz flow reactor. A diagram of the installation is presented in Fig. 1.

Methane (1) and carbon dioxide (2) were fed from a gas cylinder fitted with micrometric flow control valves (3). The flows of the gasses were measured with flow meters (4). Both reagents had been mixed in a stirrer (5) before their samples were taken for analysis (6). The gasses were fed into a quartz reactor (8) with an inside diameter of 11 mm. The catalyst bed (9) was located inside the reactor. A resistance furnace (10) was used as a heat source. Temperature was measured and controlled (12) using a control unit equipped with a digital meter and Fe-CuNi

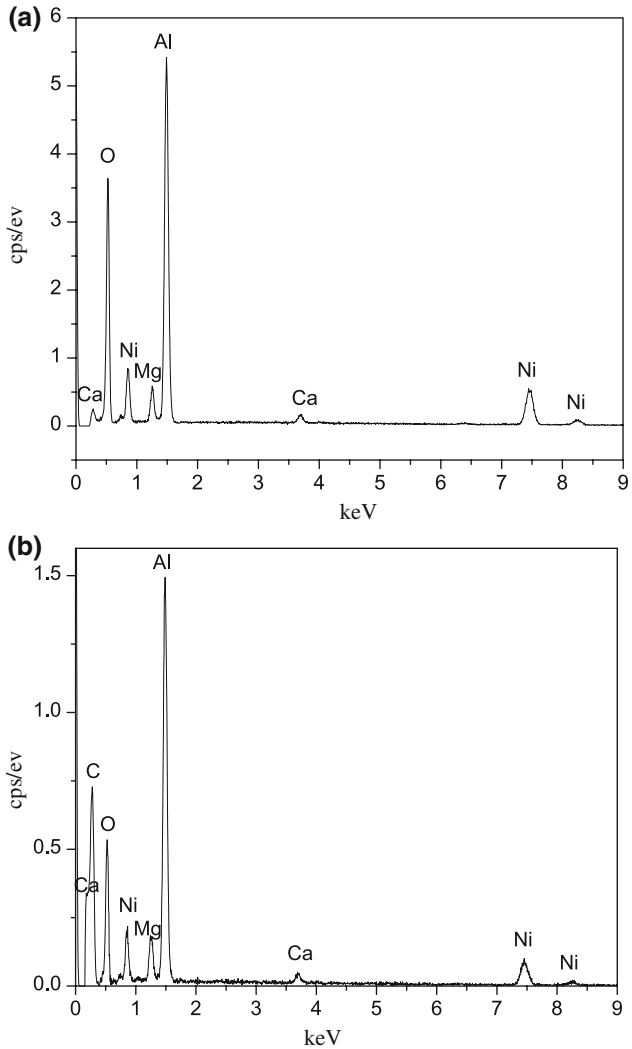

Fig. 5 The EDS X-ray spectrum of Ni industrial catalyst **a** before and **b** after reaction (550 °C)

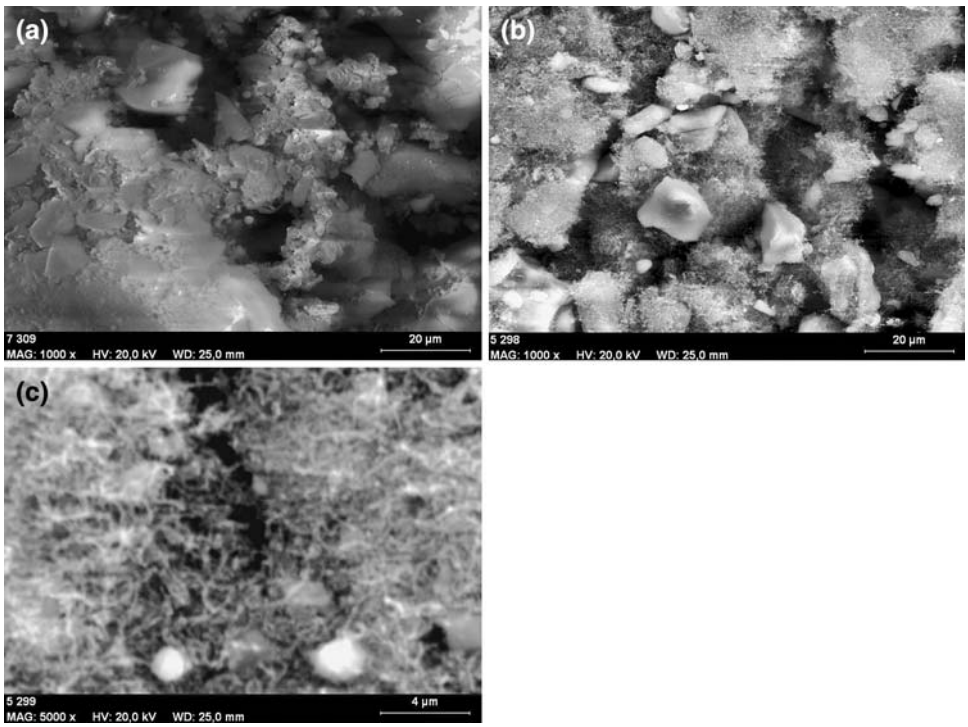

Fig. 6 SEM picture of Ni/SiO_2 catalyst **a** before, **b** after reaction (at 550 °C) taken at magnification of ×1000, **c** after reaction (at 550 °C) taken at magnification of ×5000

thermocouple (11). Gas products were taken by syringe to the GC analysis through the membrane (13) and later they were fed into ventilation system (14).

The reaction mixture consisting of methane and carbon dioxide in the mole ratio of 1:1 was introduced into the reactor at a total gas flow of 200 ml/min. CH_4/CO_2 reforming was carried out in a temperature range of 490–550 °C, at a contact time of 0.82 s (GHSV = 4,369 1/h).

The substrates and products were analyzed by means of a gas chromatography method using SRI 8610C chromatograph equipped with a thermal conductivity detector. Nitrogen and hydrogen were used as the carrier gases. Hydrogen, methane and carbon monoxide were determined on a column 1.5 m in length and with $\phi = 3$ mm filled with 5A molecular sieves operating at 40 °C, whereas carbon dioxide was determined on a column 1 m in length and with $\phi = 3$ mm filled with Poropak T operating at 40 °C.

The determination of methane and carbon dioxide conversions and hydrogen and carbon monoxide yields were calculated as follows:

$$\text{CH}_4 \text{ conversion } (\%) = \frac{(\text{CH}_4)_{\text{in}} - (\text{CH}_4)_{\text{out}}}{(\text{CH}_4)_{\text{in}}} \times 100$$

$$\text{CO}_2 \text{ conversion } (\%) = \frac{(\text{CO}_2)_{\text{in}} - (\text{CO}_2)_{\text{out}}}{(\text{CO}_2)_{\text{in}}} \times 100$$

$$\text{H}_2 \text{ yield } (\%) = \frac{(\text{H}_2)_{\text{out}}}{(\text{CH}_4)_{\text{in}}} \times \frac{100}{2}$$

$$\text{CO yield } (\%) = \frac{(\text{CO})_{\text{out}}}{(\text{CH}_4)_{\text{in}} + (\text{CO}_2)_{\text{in}}} \times 100.$$

$(CH_4)_{in}$, mole CH_4 in inlet; $(CH_4)_{out}$, mole CH_4 in outlet; $(CO_2)_{in}$, mole CO_2 in inlet; $(CO_2)_{out}$, mole CO_2 in outlet; $(CO)_{out}$, mole CO in outlet; $(H_2)_{out}$, mole H_2 in outlet

3 Results and Discussion

Table 2 presents the surface area and volume of the pores of the nickel catalysts before and after reforming of CH_4 with CO_2.

The surfaces area (S_{BET}) of prepared nickel catalysts significantly differed from the surfaces of an industrial nickel catalyst. The industrial nickel catalyst tested during the process of dry reforming had the smallest surface area among all the tested catalysts which amounted to only 4.5 m^2/g. Although the catalyst's surface area was no large, this fact had no influence on the industrial catalyst's high activity. Nickel systems deposited on the silica had a well developed surface area, which on average amounted to 297 m^2/g. The surface area of the catalysts prepared by us was reduced after the reforming CH_4. The volume of the pores of the prepared catalysts was significantly larger than that of the pores of the industrial nickel catalyst.

The nickel catalysts were investigated by means of XRD method before and after the reforming of CH_4

with CO_2. Figure 2 presents the diffraction patterns of the catalysts prepared before and after the reaction conducted at 550 °C. Figure 3 shows the XRD of industrial catalyst.

Analyzing the X-ray diffraction patterns of industrial catalyst we focused only on the patterns of carbon, nickel oxide instead of detailed phase composition analysis.

X-ray diffraction patterns of NiO were found to be identical to the reference patterns reported in the literature ($2\theta = 37.3°$ at 43.3° and 62.8° JCPDS 73-1523). The diffractograms of Ni(10)–Cu(3)/SiO_2 and Ni(10)–Cu(1)/SiO_2 show no lines of copper oxide or other compounds of this element due to too low Cu content in the catalyst.

In all the XRD patterns of post-reaction catalysts there is a characteristic peaks assigned to graphite ($2\theta = 26.2$, JCPDS 03-0401). On the basis of the intensity of this reflex it can be assumed that an increase of Cu content leads to a decrease of the amount of carbon deposit.

During the process of dry reforming a catalyst also undergoes some chemical changes. Lines assigned to NiO disappear. On the other hand some new reflexes seem to appear at both 44.2° and 51.8° which could be attributed to either nickel oxide reduction to nickel (JCPDS 04-0850) or to the formation of nickel carbide (NiC) (JCPDS 14-0020). On the basis of ICDD reference files it was ascertained that the XRD spectra of nickel and NiC are nearly identical and it is impossible to tell them apart.

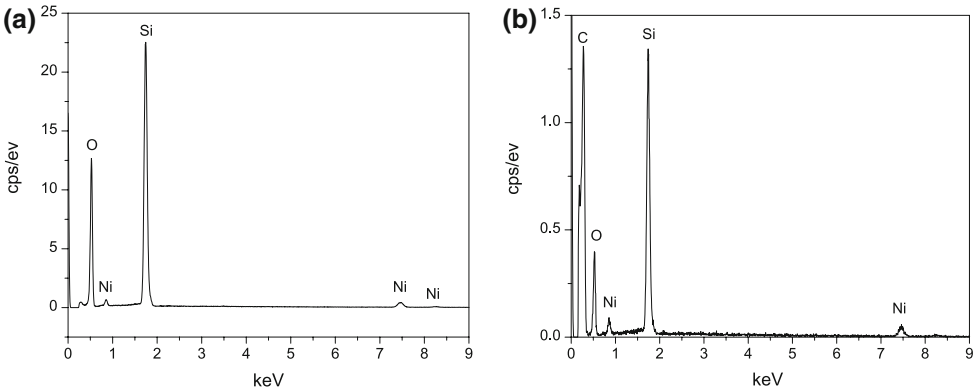

Fig. 7 The EDS X-ray spectrum of Ni/SiO_2 catalyst **a** before and **b** after reaction (550 °C)

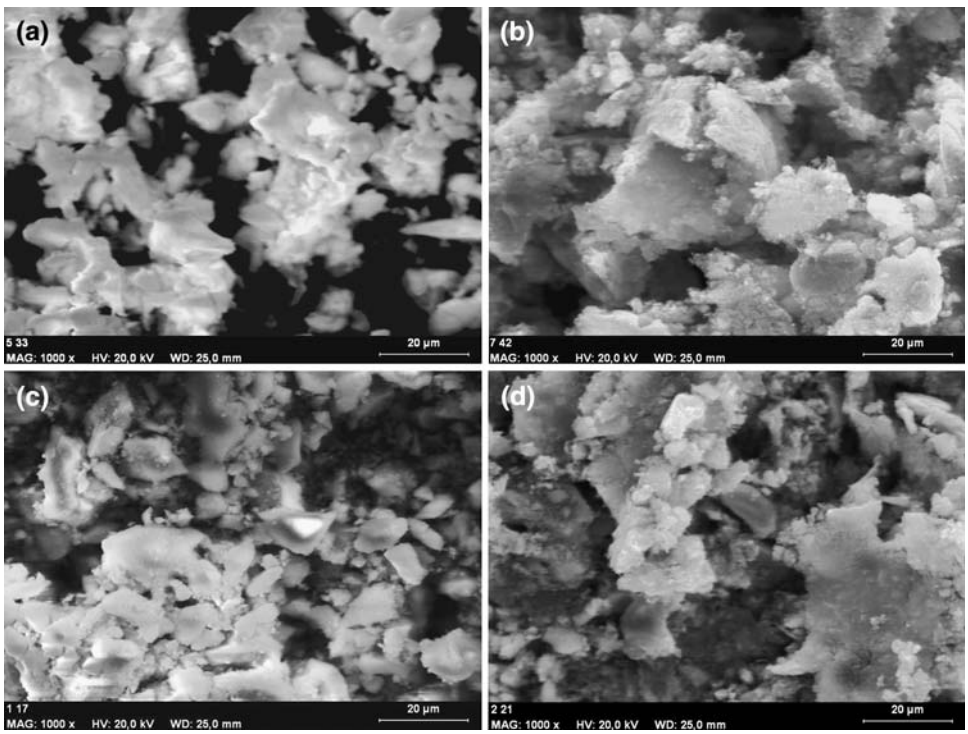

Fig. 8 SEM picture of Ni(10)–Cu(1)/SiO_2 catalyst **a** before, **b** after reaction (at 550 °C) and Ni(10)–Cu(3)/SiO_2 catalyst **c** before, **d** after reaction (at 550 °C) taken at magnification of ×1000

Figure 4 shows SEM images of an industrial nickel catalyst both before and after the reaction of methane with CO_2 performed at 550 °C.

On the surface of the catalyst after the reaction some clusters of small carbon fibers were to be seen. The presence of carbon was also confirmed using EDS method (Fig. 5). An appearance of carbon leads to a decrease of other elements' contents at the surface layers of the catalyst.

Figure 6 presents SEM images of Ni/SiO_2 catalyst. Even at 1000× magnification some clusters of carbon fibers are very clearly seen. They are much more unfolded than the fibers found on the industrial catalyst. This can be very clearly seen at 5000× magnification. The places on the surface where carbon deposit can be found are completely covered by a tangle of carbon fibers, which makes it difficult, or even impossible, for methane and carbon dioxide to come into contact with the active phase of the catalyst (Fig. 7).

An analysis of the Ni/SiO_2 surface by means of EDS method has confirmed a significant depletion of the surface layers, especially as far as nickel and silicon compounds were concerned.

The analyses of the morphology of spent bimetallic nickel-copper catalysts on SiO_2 carrier performed by means of SEM method (Fig. 8) showed that on the surface of these samples there was a significantly smaller amount of carbon deposit on comparison to Ni/SiO_2 catalyst. An increase of copper content lead to a decrease of carbon formation. Carbon is observed in the form of small clusters of minute carbon fibers, which on the catalyst with 3% copper content are difficult to see. The presence of carbon has been confirmed using EDS method (Fig. 9).

Table 3 shows CH_4 and CO_2 conversions and CO and H_2 yields, at 550 °C and at a stationary state.

Over Cu contained catalysts the methane and CO_2 conversions as well as CO and H_2 yields are stable from the start of the reaction. The activity of the nickel catalysts increases slightly at the start of the reaction, probably because of an activation of the catalysts. After 30 min, a stable and rather significant conversion of CH_4 takes place producing large quantities of H_2.

The best methane conversion (57%) and H_2 (53%) yield were achieved over Ni industrial catalyst. Whereas the best CO (5%) yield was achieved over $Ni(10)–Cu(1)/SiO_2$ catalyst. Very similar values of CO_2 conversion and CO yield were obtained in all the investigated systems.

What is surprising is a relatively high ratio of hydrogen to carbon monoxide, which in the industrial nickel catalyst was almost 14. This is probably due to the fact that Boudouard reaction was also taking place.

Table 3 Catalytic activity of Ni/SiO_2, $Ni–Cu/SiO_2$ catalysts and industrial Ni catalyst in the methane dry reforming with carbon dioxide at 550 °C after 5 h reaction

Catalysts	Conversion (%)		Yield (%)		H_2/CO
	CH_4	CO_2	H_2	CO	
$Ni(10)/SiO_2$	42	34	40	4.7	8
$Ni(10)–Cu(1)/SiO_2$	23	43	20	5	4
$Ni(10)–Cu(3)/SiO_2$	28	34	24	4	5.6
Ni industrial	57	36	53	4	13.8

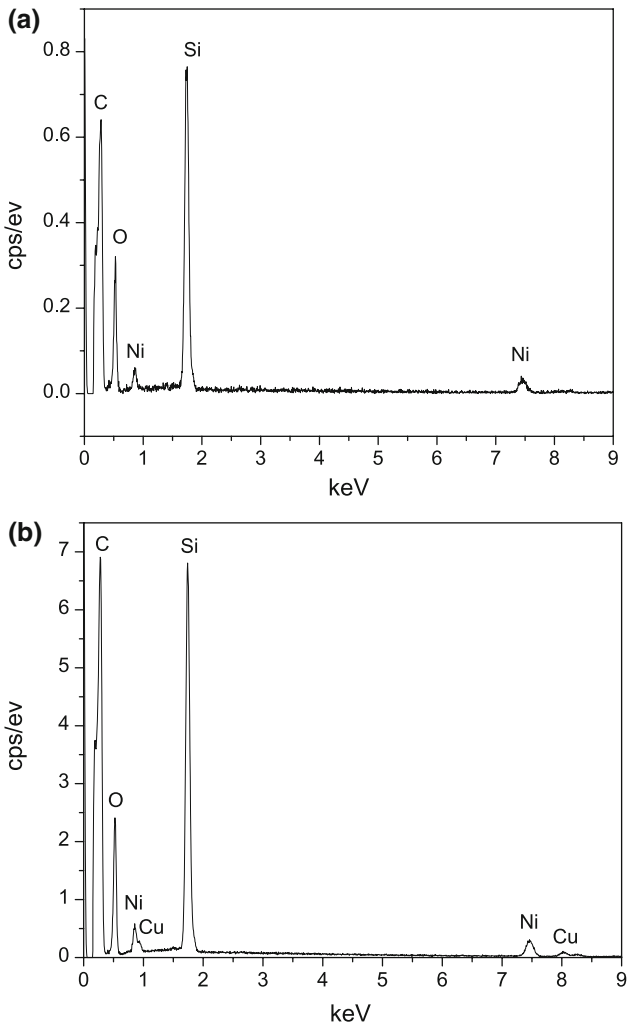

Fig. 9 The EDS X-ray spectrum of **a** $Ni(10)–Cu(1)/SiO_2$ and **b** $Ni(10)-Cu(3)/SiO_2$ catalyst after reaction (550 °C)

$$2CO \rightleftarrows C + CO_2 \quad \Delta H = -172\,kJ/mol \tag{3}$$

4 Conclusions

An industrial nickel catalyst used in the traditional method of synthesis gas production can also be used in dry

reforming. However, it undergoes deactivation as a result of carbon formation. The amount of carbon deposit is in this case significantly smaller than that on a prepared catalyst (Ni/SiO_2), but larger than that on catalysts containing copper. An addition of copper inhibits the speed of carbon formation on the catalyst. A modification of an industrial catalyst through copper addition can increase the catalyst's resistance toward carbon deposition.

References

1. Jeong H, Kim K (2006) J Mol Catal A 246:43
2. Nandini A, Pant KK, Dhingra SC (2005) Appl Catal A 290:166
3. Xiancai L, Min W, Zhihua L, Fei H (2005) Appl Catal A 290:81
4. Tomiyama S, Takahashi R, Sato S, Sodesawa T (2003) Appl Catal A 241:349
5. Bouarab R, Akdim O, Auroux A, Cherifi O, Mirodatos C (2004) Appl Catal A 264:161
6. Wang S, Lu GQM (1998) Appl Catal A 16:269
7. Wang S, Lu GQ (1998) Appl Catal A 169:271
8. Lee J, Lee E, Joo O, Jung K (2004) Appl Catal A 269:1
9. Juan-Juan J, Roman-Martinez MC, Illan-Gomez MJ (2004) Appl Catal A 264:169
10. Takanabe K, Nagaoka K, Nariai K, Aika K (2005) J Catal 232:268
11. Takanabe K, Nagaoka K, Nariai K, Aika K (2005) J Catal 230:75
12. Naganka K, Takanabe K, Aika K (2004) Appl Catal A 268:151
13. Naganka K, Takanabe K, Aika K (2003) Appl Catal A 255:13
14. Choudhary VR, Mondal KC, Choudhary TV (2006) Ind Eng Chem Res 45:4597
15. Ruckenstein E, Wang HY (2001) Appl Catal A 204:183
16. Wang HY, Ruckenstein E (2001) Appl Catal A 209:207
17. Souza MMVM, Schmal M (2003) Appl Catal A 255:83
18. Ferreira-Aparicio P, Fernandez-Garcia M, Guerrero-Ruiz A, Rodriguez-Ramos I (2000) J Catal 190:296
19. Portugal UL, Marquez CMP, Araujo ECG, Morale EV, Giotto MV (2000) Appl Catal A 193:173
20. Sharma S, Hilaire S, Gorte RJ (2000) Stud Surf Sci Catal 130:677
21. Nagaoka K, Sheshan K, Aika K, Lercher JA (2001) J Catal 197:34
22. Kim J-H, Suh DJ, Park T-J, Kim K-L (2000) Appl Catal A 197:191
23. Chen H-W, Wang C-Y, Yu C-H, Tseng L-T (2004) Catal Today 97:173
24. Pietri E, Barrios A, Goldwasser MR (2000) Stud Surf Sci Catal 130:3657
25. Quincoces CE, de Vargas SP, Gonzalez MG (2000) Stud Surf Sci Catal 130:3651
26. Crisafulli C, Scire S, Maggiore R, Minico S, Galvagno S (1999) Catal Lett 59:21